A Study on the Prevention of Cracks on the Trepan Area of Motor Bearing

Kyung Won Lee, Jae Sam Ban, Heyong Seon Kang, Kyu Zong Cho*
Department of Mechanical Engineering, Chonnam National University, Gwangju 500-757, Korea

Trepan prevents the wear of the inside part of a bearing when the initial shaft rotates. It continuously contacts with the eccentric part of the shaft in rotation and is loaded repeatedly. Therefore, even if an early crack of a trepan part is small, the crack may progress by the repeated load. If the crack progresses, very small chips come out. This is put in the rotor and prevents the rotation of the compressor. There can be leaks in a microgroove and extreme wear can occur due to lack of oil on the surface contact part. Therefore, this study was carried out to compare and investigate the trepan strength and deflection characteristics between trepan locations and dimension changes using the finite element method and search a motor bearing for a model with bigger stiffness of a trepan part and the same deflection.

Key Words : Motor Bearing, Trepan, Finite Element Analysis, Stress, Deflection

Nomenclature

Z_1 : Location of the main bearing force in the "z" direction
Z_2 : Location of the secondary bearing force in the "z" direction
Z_{rot} : Location of the rotor weight force in the "z" direction
F_{bg1} : Main bearing force
F_{bg2} : Secondary bearing force
F_{ec} : Eccentric force
H_r : Height of roller
H_{rot} : Height of rotor
L_{bg1} : Length of main bearing
L_{bg2} : Length of secondary bearing
THF_{bg1} : Angular position of the main bearing
THF_{bg2} : Angular position of the secondary bearing force
W_{rot} : Rotor weight force

* Corresponding Author,
E-mail : kzcho@chonnam.ac.kr
TEL : +82-62-530-1663; **FAX** : +82-62-530-1689
Department of Mechanical Engineering, Chonnam National University, Gwangju 500-757, Korea. (Manuscript **Received** May 2, 2002; **Revised** October 5, 2002)

1. Introduction

The compressor is used under high pressure. It compresses vapor so that the refrigerant vaporized in a vaporizer is easily condensed. The refrigerant condenses and vaporizes repeatedly by working through the vaporizer and circulates inside the refrigerating device and carries heat. Compared with a human body, the refrigerant is like the blood and the heart circulates the blood. The compressor of a refrigerant device is the heart of the refrigerant device. The bearing is an important element of the compressor. Studies that have been undertaken so far include: an optimum design of dynamically-loaded journal bearings by mobility method (Shim et al., 1986), the cavitation in a journal bearing with pressurized lubricant supply (Kim et al., 1986), theoretical simulation and experimental evaluation of an hermetic rolling piston rotary compressor (Krueger, 1988), a finite element model of asymmetrical rotor-bearing systems (Jei et al., 1988), an optimal design of the crank press main journal bearing (Shim et al., 1989), an analysis of the circumferentially grooved floating ring journal

bearing (Cheong et al., 1991), residual stress analysis of an external grooved thick-walled pressure vessel (Koh, 1993), the static and stability characteristics of the oil-lubricated herringbone groove journal bearing (Kang et al., 1998), relation between correction masses and bearing forces in a rigid rotor (Jun, 1999), an analysis of herringbone groove journal bearing considering groove shape (Shin et al., 2000), crack detection, localization and estimation of the depth in a turbo rotor (Park, 2000), mixing flow effects in a high-speed journal bearing (Chun et al., 2001), experimental testing of journal bearings with two-component surface layer in the presence of an oil abrasive contaminant (Jaroslaw Sep et al., 2001), optimum design of short journal bearings by artificial life algorithm (Yang et al., 2001), on the performance of dynamically loaded journal bearings lubricated with couple stress fluids (Wang et al., 2002), a parametric study on bubbly lubrication of high-speed journal bearings (Chun, 2002).

A crack occurrence in the trepan part of a motor bearing, which is a part of the compressor, has an effect on the productivity in industrial spots. If a crack occurs in the trepan part, this part is disposed. And, if a crack occurs in the trepan part, it takes many hours to inspect a machine and select inferior goods that may be mixed.

Trepan prevents the wear of the inside part of a bearing when the initial shaft rotates but contacts continuously with the eccentric part of rotating shaft and is loaded repeatedly. Therefore, even if an early crack of a trepan part is small, the crack may progress by the repeated load. If the crack progresses, very small chips come out. This is put in the rotor and prevents rotating of a compressor. A leak may occur in a microgroove and cause extreme wear due to lack of oil on the surface contact part.

Therefore, this study is to compare and investigate the trepan strength and deflection characteristics between trepan locations and dimension changes using the finite element method and then search a motor bearing for a model with bigger stiffness of a trepan part and the same deflection for the prevention of cracks on the trepan area. Base trepan now in production is modeled and analyzed using the finite element method. Reliability on the finite element analysis is secured by comparing experiment data. The finite element analysis is carried out with a modified trepan.

2. Numerical Analysis

2.1 Modification of trepan

2.2.1 Load theory of the performance analysis

The locations of bearing forces and rotor weight force are given by;

$$Z_1=\frac{(H_r+L_{bg1})}{2}\hat{k} \tag{1}$$

$$Z_2=\frac{(H_r+L_{bg2})}{2}\hat{k} \tag{2}$$

$$Z_{rot}=\frac{(2L_{bg1}+H_r+H_{rot})}{2}\hat{k} \tag{3}$$

From the force and moment balance the bearing forces can be evaluated. The resulting equations are;

$$F_{bg1}\hat{i}=-F_{ec}\hat{i}\frac{Z_2}{Z_2-Z_1} \tag{4}$$

$$F_{bg2}\hat{i}=-F_{bg1}\hat{i}\frac{Z_1}{Z_2} \tag{5}$$

$$F_{bg1}\hat{i}=(W_{rot}\hat{i}\frac{(Z_2-Z_{rot})}{Z_2}-F_{ec}\hat{i})\left(\frac{Z_2}{Z_2-Z_1}\right) \tag{6}$$

$$F_{bg2}\hat{i}=\frac{Z_{rot}W_{rot}\hat{i}-Z_1F_{bg1}\hat{i}}{Z_2} \tag{7}$$

The magnitude and the angular position of the bearing forces are (Krueger, 1988);

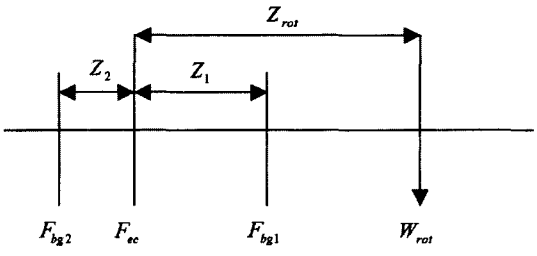

Fig. 1 Rotor-shaft free body diagram

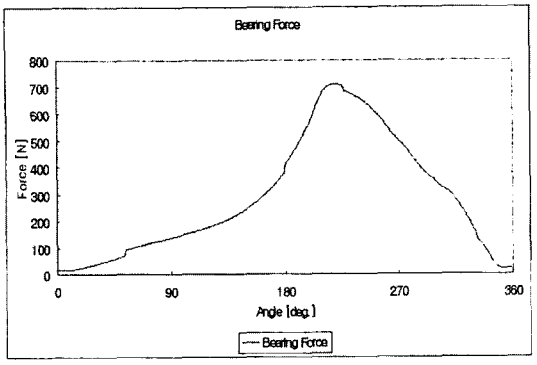

Fig. 2 Force applied to bearing

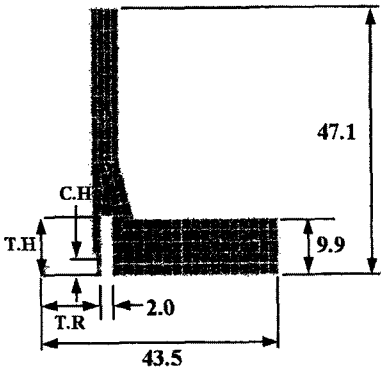

Fig. 3 Dimension of trepan

$$F_{bg1}=\sqrt{(F_{bg1}\hat{i})^2+(F_{bg1}\hat{j})^2} \quad (8)$$

$$F_{bg2}=\sqrt{(F_{bg2}\hat{i})\,(F_{bg2}\hat{j})^2} \quad (9)$$

$$THF_{bg1}=a\tan 2(F_{bg1}\hat{i},\ F_{bg1}\hat{i}) \quad (10)$$

$$THF_{bg2}=a\tan 2(F_{bg2}\hat{i},\ F_{bg2}\hat{i}) \quad (11)$$

Figure 1 presents a rotor shaft free body diagram with a load.

A numerical analysis was carried out following the load theory based on the performance analysis. Loads were found in each angle. Figure 2 is a graph for the load found at this time. Here, the graph curve is only a load which influences the trepan.

2.2.2 Finite element analysis

Figure 3 is a model of the section (1/2) of a motor bearing and presents a dimension of the trepan where C.H is the chamfer location, T.H is the trepan depth, and T.R is the trepan location. After the section of the two dimensional figure changes into a three dimensional section, an analysis is carried out using the commercial program, ANSYS. The elastic modulus, E is 110 GPa and Poisson's ratio, v is 0.3 and the density, ρ is 650 kgf/m^3. The load on the bearing is found using the numerical analysis, following the load theory based on the performance analysis.

Figure 4 presents the boundary condition, the constraint and the loading condition of a motor bearing. In Fig. 4, constraint is applied to the parts of fixed bolts and load applied to a bearing.

Figure 5 is a result from the finite element analysis and is a good representation of a stress concentration part of trepan and deflection.

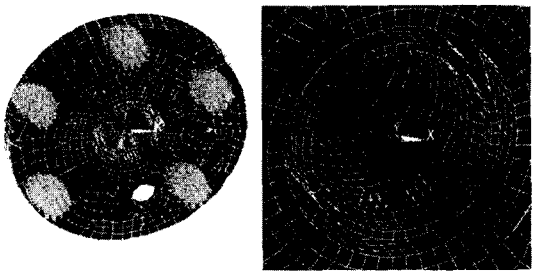

Fig. 4 Boundary condition of motor bearing

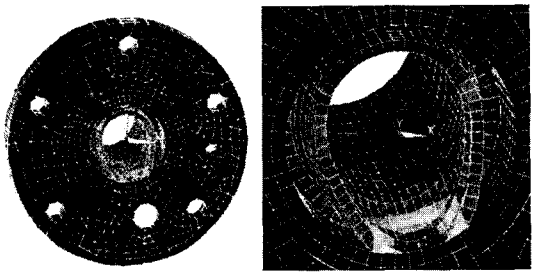

Fig. 5 FEM analysis of motor bearing

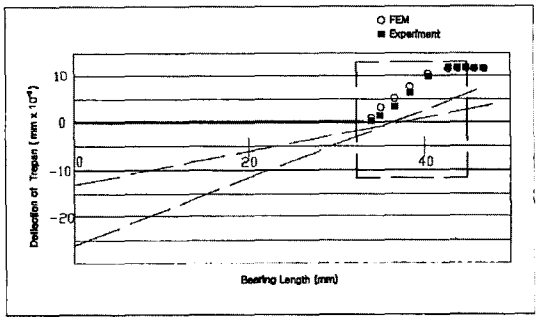

Fig. 6 Deflection of trepan

Figure 6 is a graph in which experimental data of base trepan is compared with the results from the finite element analysis on deflection of trepan. Here, it is very difficult to measure deflection of trepan by the eccentric part of the shaft in rotating. Therefore, the load was added to a stationary shaft to measure deflection of trepan. Figure 6 presents that the experiment data of base trepan show the same results from the finite element analysis. Therefore, there is secured reliability on the finite element analysis.

First, if the base model of Fig. 7 is compared with the model 1 of Fig. 8, the model 1 is 0.5 mm longer than the base model for crack prevention. From the results of the finite element analysis, the deflection of base model is 11.9 μm and stress is 62.7 MPa. The deflection of model 1 is 8.2 μm and stress is 44.8 MPa. Shape modification is needed because the deflection of model 1 is shorter than the deflection of the base model.

Therefore, after modifying only the chamfer location from 3.6 mm to 2.0 mm as shown in Fig. 9, the finite element analysis is carried out.

From the results of the finite element analysis on the model 2 of Fig. 9, deflection is 11.1 μm and stress is 63.4 MPa. That is shorter than the deflection of the base model and bigger than the stress of the base model. It is found that the shorter the chamfer location is, the smaller the stress is. Therefore, thickness is lengthened by 0.5 mm and depth increasing by 1 mm in leaving as the chamfer is.

From the results of the finite element analysis on the model 3 of Fig. 10, deflection is 9.7 μm and stress is 50.6 MPa. The deflection was longer by 1.5 μm and stress increased by 5.8 MPa than those of model 1. Stress increased by 5.8 MPa, but that is smaller than the stress of the base model, 62.7 MPa. Therefore, that is the allowed value.

From the results of the finite element analysis

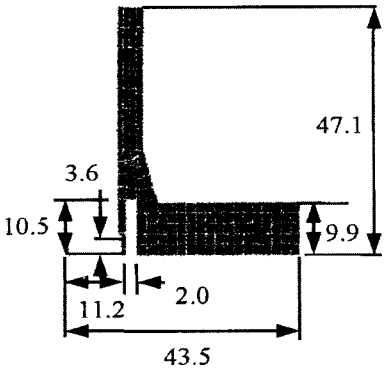

Fig. 7 Base model

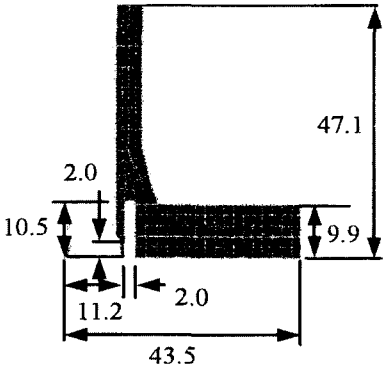

Fig. 9 Modification model 2

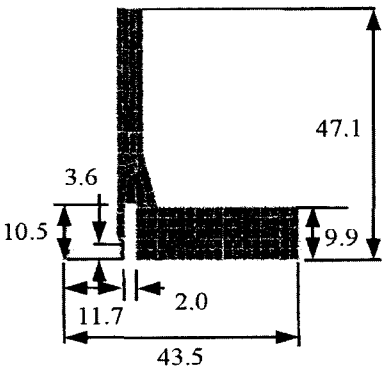

Fig. 8 Modification model 1

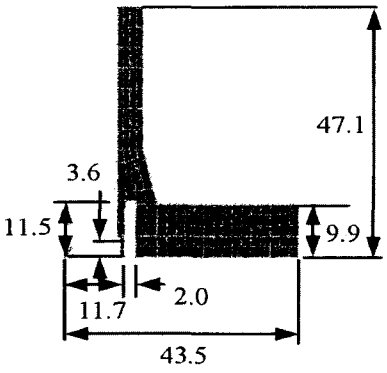

Fig. 10 Modification model 3

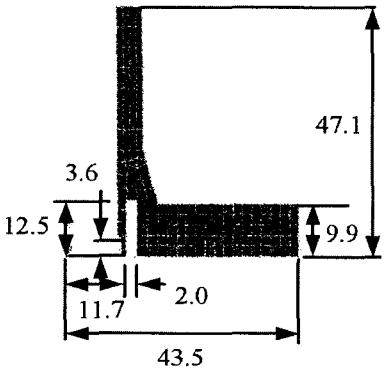

Fig. 11 Modification model 4

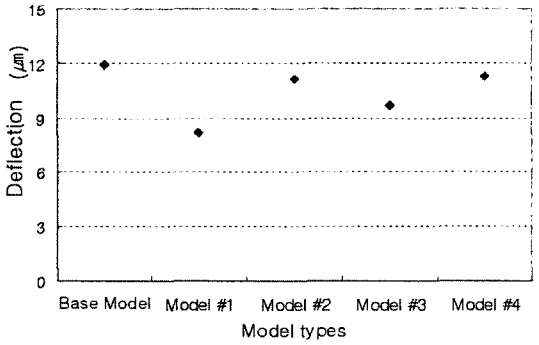

Fig. 12 Deflection analysis result

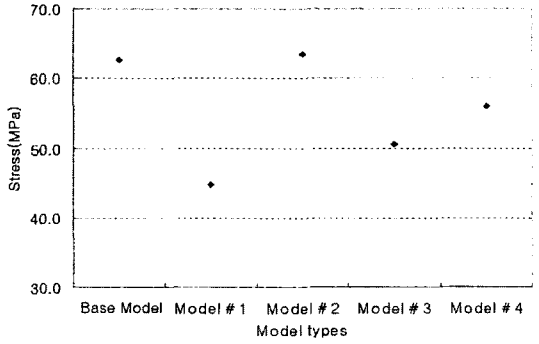

Fig. 13 Stress analysis result

on the model 4 of Fig. 11, deflection is 11.3μm and stress is 55.9 MPa. The deflection was longer by 1.6 μm and stress increased by 5.3 MPa than those of the model 3. Stress decreased by 6.8 MPa than the stress of the base model. Deflection is most similar to the deflection of the base model. Therefore, it is suitable to exchange the model 4 for the base model.

Figure 12 is the table for the deflection analysis results using the finite element analysis in each modification model.

Figure 13 is the table for the stress analysis results using the finite element analysis in each modification model.

3. Conclusion

The trepan shape was modified to prevent cracks on the trepan area of motor bearing and the finite element analysis was carried out.

The results are summarized as follows :

(1) An experiment data of the base trepan demonstrated the same results from the finite element analysis. Therefore, there is secured reliability on the finite element analysis.

(2) The thicker the thickness of the trepan is than that of the base model, the smaller the stress is as well as the deflection is also.

(3) The shorter the chamfer location of trepan is than that of the base model, the smaller the stress is as well as the deflection is also.

(4) The stress is smaller than that of the base model and the deflection is the most similar to the deflection of the base model when increasing the thickness of the trepan along with a 2 mm depth.

Acknowledgment

The authors would like acknowledge the financial support from the BK21 for conduction this research work.

References

Cheong, Y. M. and Kim, K. W., 1991, "An Analysis of the Circumferentially Grooved Floating Ring Journal Bearing," *Journal of the KSLE*, Vol. 7, No. 2, pp. 75~84.

Chun, S. M. 2002, "A Parametric Study on Bubbly Lubrication of High-Speed Journal Bearings," *Tribology International*, Vol. 35, No. 1, pp. 1~13.

Chun, S. M. and Ha, D. H., 2001, "Study on Mixing Flow Effects in a High-Speed Journal Bearing," *Tribology International*, Vol. 34, Issue 6, pp. 397~405.

Jaroslaw Sep, Anna Kucaba-Pietal, 2001, "Experimental Testing of Journal Bearings with Two-component surface Layer in the Presence of an Oil Abrasive Contaminant," *Wear*, Vol. 249, No. 12, pp. 1090~1095.

Jei, Y. G. and Lee, C. W., 1988, "Finite Element Model of Asymmetrical Rotor-Bearing Systems," *KSME Int. J.*, Vol. 2, No. 2, pp. 116~124.

Jun, O. S., 1999, "Relation Between Correction Masses and Bearing Forces in a Rigid Rotor," *KSME Int. J.*, Vol. 13, No. 11, pp. 791~797.

Kang, K. P. and Rhim, Y. C., 1998, "A Study on the Static and Stability Characteristics of the Oil-Lubricated Herringbone Groove Journal Bearing," *J. KSME A*, Vol. 22, No. 4, pp. 859~867.

Kim, K. W. and Moon, W. S., 1986, "A Study on the Cavitation in a Journal Bearing with Pressurized Lubricant Supply," *Journal of the KSLE*, Vol. 2, No. 2, pp. 44~51.

Koh, S. K., 1993, "Residual Stress Analysis of an External Grooved Thick-Walled Pressure Vessel," *KSME Int. J.*, Vol. 7, No. 3, pp. 194~202.

Manfred Krueger, 1988, "Theoretical Simulation and Experimental Evaluation of An Hermetic Rolling Piston Rotary Compressor," *Purdue University*., M.S. thesis.

Park, R. W., 2000, "Crack Detection, Localization and Estimation of the Depth in a Turbo Rotor," *KSME Int. J.*, Vol. 14, No. 7, pp. 722~729.

Shim, H. H., Kim, C. H., Oh, P. K. and Kwon, O. K., 1986, "Optimum Design of Dynamically-Loaded Journal Bearings by Mobility Method," *Journal of the KSLE*, Vol. 2, No. 2, pp. 32~43.

Shim, H. H., Kim, C. H. and Kwon, O. K., 1989, "Optimal Design of the Crank Press Main Journal Bearing," *KSME Int. J.*, Vol. 5, No. 1, pp. 69~75.

Shin, D. W. and Rhim, Y. C., 2000, "An Analysis of Herringbone Groove Journal Bearing Considering Groove Shape," *Journal of the KSLE*, Vol. 16, No. 6, pp. 425~431.

Wang, X. L., Zhu, K. Q. and Wen, S. Z., 2002, "On the Performance of Dynamically Loaded Journal Bearings Lubricated with Couple Stress Fluids," *Tribology International*, Vol. 35, No. 3, pp. 185~191.

Yang, B. S., Lee, Y. H., Choi, B. K. and Kim, H. J., 2001, "Optimum Design of Short Journal Bearings by Artificial Life Algorithm," *Tribology International*, Vol. 34, No. 7, pp. 427~435.